3rd URSI AT-AP-RASC, Gran Canaria, 29 May – 3 June 2022

Microwave Microfabricated Sensor Dedicated to the Dielectric Characterization of Biological Microtissues

Olivia Peytral-Rieu(1), David Dubuc(1), and Katia Grenier(2)
(1) LAAS-CNRS, Université de Toulouse, CNRS, UPS, Toulouse, France
(2) LAAS-CNRS, Université de Toulouse, France

Abstract

Microwave dielectric spectroscopy is a promising technique that allows intracellular, non-invasive, label-free and cost-effective biological studies. To complement the sensing possibilities of this technique at this frequency range, which have been previously demonstrated at the single cell, cellular suspensions and organs levels, a microwave-based sensor is designed, fabricated and evaluated to dielectrically characterize 3D biological microtissues. Such a biological model is indeed of high interest for biological investigations, as it constitutes an intermediate entity between 2D cell cultures and organs, exhibiting a biological response close to the one obtained with tissue physiology. The proposed sensor here the development of one of the first microfabricated device for spheroids studies. A discussion on the way of analyzing the data is proposed thanks the measurements of different fixed spheroids and polystyrene beads.

1. Introduction

Electrical approaches, especially dielectric spectroscopy, have been proven to be useful for a broad range of research purposes including biological researches [1], [2] as it they are non-invasive and non-destructive. These techniques use the interaction between electromagnetic fields and materials for biological investigations, while being label-free and cost-effective [3], [4]. Among these techniques, the microwave dielectric spectroscopy, attracts increasing attention, as its frequency range enables intracellular investigations. This ability is indeed due to the fact that electromagnetic waves may by-pass the capacitive cellular membrane, giving access to the interior of cells. Previous investigations on microwave dielectric spectroscopy demonstrated the possible detection of various molecules such as amino acids, carbohydrates, proteins, or nucleic acids in aqueous solutions, as well as cells in solutions [5]–[7], at the individual cell level and with organs [8]–[10]. It may also provide different dielectric properties depending on chemically or electrically based stimuli applied to cells or yeasts. It therefore makes this analyzing technique as a promising method for drug testing notably [11], [12]. So far, another important biological model is still missing from the analyzing arsenal of microwave dielectric spectroscopy. 3D cell aggregates (also called spheroids or micro-tissues) constitutes however a well-established model, which is located in-between the *in vivo* and the 2D *in vitro* cell culture models. In addition to mimicking the particular defense of genuine tumors through bio-mechanisms, they present a convenient array of advantages for accurate studies. They present i) a quick maturation time, ii) reduced production costs, iii) *in vivo*-like configurations in terms of complexity, size and organization [13]. For example, when microtissues exhibit diameters greater than 200 µm, they present an onion configuration with different layers. A hypoxic internal core is formed (composed of dead or dying cells) due to the limited oxygen diffusion allowed by the upper cell layers, whereas the external layer present healthy cells. This may notably lead to the triggering of the differentiation of certain cells among the different spheroid cell layers, making the external layer cells invasive for instance [14]. Different microwave-based sensors have already been defined for the analysis of biological objects ranging from individual cells to entire organs of patients [8], [15]–[17]. However, there is a gap in the literature for the study of mid-size microtissues with microwave dielectric spectroscopy. Here, a microfabricated device dedicated to the microwave characterization of such microtissues is introduced. It enables to fill the gap previously mentioned by characterizing the dielectric properties of spheroids with the extraction of capacitive and conductive contrasts for first polystyrene beads and then fixed spheroids. The microfabrication of this device is presented and maintained simple due to an appropriate design, which allies both microwave and fluidic considerations and constraints.

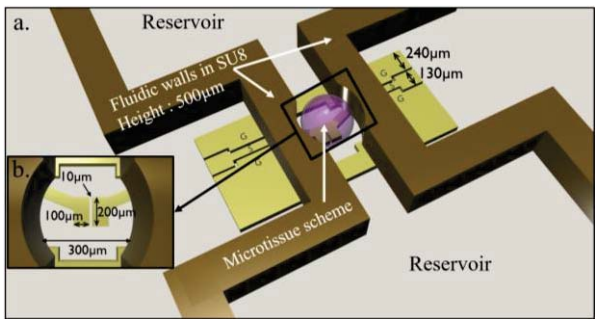

Figure 1. Scheme of the miniature sensor dedicated to the microwave characterization of a spheroid. (a) Global scheme; (b) zoom vision of the black square in the middle of the device.

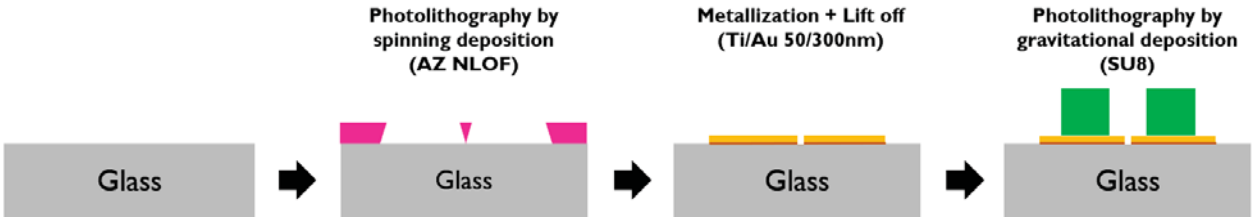

Figure 2: Microfabrication flow diagram of the biosensor with, in pink, the representation of the NLOF photoresist, in yellow, the conductive layer in gold, in brown, its adhesion titanium layer, and in green, a thick and patterned SU-8 polymer layer.

2. Materials & Methods

2.1 The studied object: fixed spheroids

Multicellular three-dimensional (3D) tumor spheroids are recognized as superior models for the preclinical evaluation of anti-cancer therapies due to their better and more advanced representation of *in vivo* tumors. The organization of cells within the 3D spheroidal structure means that they are in direct contact with each other and the secreted extracellular matrix (ECM), allowing them to utilize alternative cell growth and survival signaling mechanisms not readily observed in 2D monolayers [18], [19]. This study is employing microtissues constituted of HEK293T cells. They are fixed using paraformaldehyde and stored in Phosphate Buffer Solution (Gibco Phosphate Buffered Saline 1X in our case, called PBS in the rest of this article).

2.2 Presentation of the microwave sensor and its microfabrication process

As shown with the schematic of Figure 1, the microwave biosensor is composed of a coplanar waveguide with a capacitive gap located in the center of the structure. Coplanar accesses are widened at the RF input and output to allow coplanar probe positioning with a pitch of 150µm. The size of the coplanar waveguide has been defined to exhibit a 50 Ω characteristic impedance. It also includes a capacitive gap of 10 µm width at the center of the structure. The biological entity under test is localized just above this sensing gap, within a dedicated place. The sensor also includes an open fluidic microchannel with two reservoirs placed apart. Due to the open fluidic configuration, the process only includes two mains steps, one to realize the metallic coplanar waveguide, and a second one for the fluidic part respectively. Figure 2 shows the fabrication flow diagram of the biosensor. The biosensor is fabricated on a lossless dielectric substrate (Corning Eagle XG series). The glass substrate is cleaned using a piranha bath during five minutes followed by an oxygen plasma treatment for fifteen minutes. A mask is photolithographically applied to a 2.5-µm-thick AZ NLOF-photoresists to define the biosensor electrodes structures. A Titanium and Gold (Ti/Au) layer is then deposited by evaporation. With an acetone bath applied during one hour, the NLOF photoresist is removed to obtained only the gold electrodes through a lift off process. The final step consists in the deposition by gravitation of a 500 µm thick SU8-3050 layer, which is then photopatterned and cured. This layer enables the creation of (i) the fluidic channel, where the spheroid is placed and maintained in PBS, and (ii) two fluidic reservoirs placed apart, which prevents evaporation in the fluidic channel.

2.3 Microwave measurements protocol and electrical modeling

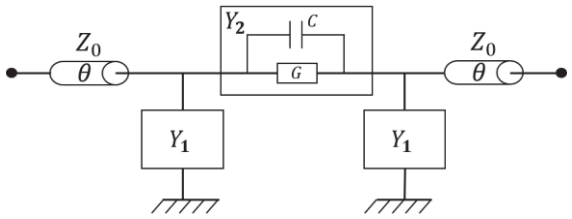

Figure 3: Electrical model of the device.

For testing, the device under test is connected to a Vector Network Analyzer using two coplanar probes and two coaxial cables. Before measurements, a preliminary SOLT calibration step is done. Microwave measurements are then performed from 500 MHz to 20 GHz. A protocol has then been established. First, the device is measured empty of any liquid or object, allowing to obtain the *S* parameters of the device itself. The liquid host medium (i.e. PBS in our case) is then loaded in the device and measured. This measurement serves afterwards as a reference one. Finally, the object under study is loaded and measured. Dielectric data are then extracted with an electrical model, which is presented in the Figure 3. Y_1 represents the admittance of the fluidic walls, Y_2 the admittance of the sensing zone above the electrodes. Parameters of interest here are the capacitance C and the conductance G. Extracted from the above-mentioned S parameters, C_{PBS} and G_{PBS}, as well as C_{SO} and C_{SO} are introduced and correspond to the electrical parameters when the device is loaded with the reference fluid or with the studied object (SO) in liquid respectively. Further details of these calculations may be found in [20]. Based on these electrical elements, capacitive and conductive contrasts are calculated between the system loaded with the studied object and the reference fluid, using equations (1) and (2) respectively. Such contrasts are used to better highlight small dielectric variations.

$$\Delta C = C_{SO} - C_{PBS} \quad (1)$$

$$\Delta G = G_{SO} - G_{PBS} \quad (2)$$

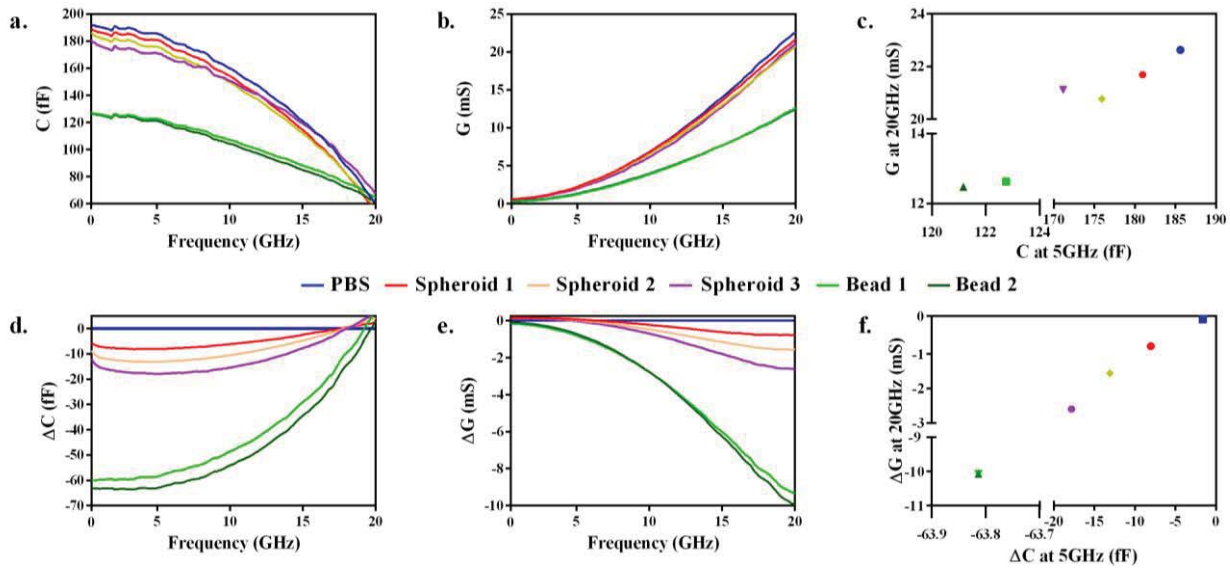

Figure 4: Measurements performed with different polystyrene beads and spheroids. Extracted (a) capacitance and (b) conductance obtained for the different objects. (c) Complex electrical representation of the capacitance and conductance, at 5 GHz and 20 GHz respectively. (d) Capacitive and (e) conductive contrasts. (f) Complex electrical representation of the capacitive and the conductive contrasts at 5 GHz and 20 GHz respectively. The tested spheroids and polystyrene beads present diameters between 200µm and 360µm.

3. Results & Discussions

To validate the sensor and verify the accuracy of the technique, measurements of two different polystyrenes beads are done first. Figure 4 presents the corresponding results in terms of capacitance and conductance versus frequency (Figure 4 a and b), as well as the capacitive and conductive contrasts (Figure 4 c and d). Due to the low permittivity of polystyrene beads close to 2.56 compare to the PBS liquid, which exhibits a permittivity close to the one of water, a large variation between the reference liquid and the beads is obtained. The extracted capacitive contrasts are close to 60 fF below 5 GHz, whereas the conductive contrasts at 20 GHz reach a value of 10 mS, in relative value. Three different fixed spheroids are then characterized. Results are also indicated in Figure 4. As expected, the differences between the spheroids and the PBS are much smaller than for the polystyrene beads. Moreover, each spheroid presents a specific dielectric response due to variations in terms of size and shape. It is indeed difficult to produce microtissues perfectly round and exhibiting the same diameter. The discrimination between the host medium and the spheroids is even weaker as they have been fixed in a formaldehyde solution. This fixation creates indeed the permeabilization of the cell membranes, leading to the equilibrium between the intracellular medium and the extracellular one [21], [22]. The consecutive contrast is consequently lower that those, which would have been reached with unfixed microtissues. The choice of such fixed spheroids is due to the fact that we were looking to establish a proof of concept, namely the first validation of the sensor to characterize 3D biological spheroids. It was consequently easier to prepare fixed spheroids, which may be stored for weeks and used at convenience for experiments. The extracted electrical contrasts are then close to the reference level (PBS corresponds to the zero level), with values ranging from 8 to 18 fF at 5 GHz for the capacitive contrast, and between 0.7 to 2.6 mS for the conductive contrast at 20 GHz.

4. Conclusions

A microfabricated device enabling the microwave characterization of microtissues is presented. It exhibits a simple fabrication process. The successful microwave measurements of both polystyrene beads and then spheroids with a diameter close to 300 µm demonstrate the possible dielectric analysis of such biological models.

5. Acknowledgements

This work was partly supported by LAAS-CNRS micro and nanotechnologies platform member of the French RENATECH network.

References

[1] R. D. Stoy, K. R. Foster, and H. P. Schwan, "Dielectric properties of mammalian tissues from 0.1 to 100 MHz; a summary of recent data," *Phys. Med. Biol.*, vol. 27, no. 4, pp. 501–513, 1982.

[2] P. Mehrotra, B. Chatterjee, and S. Sen, "EM-wave biosensors: A review of RF, microwave, mm-wave and optical sensing," *Sensors (Switzerland)*, vol. 19, no. 5, 2019.

[3] H. Thielecke, J. Fleckenstein, P. Bartholomä, and C. Rübe, "Evaluation of impedance spectroscopy for the characterization of small biological samples in tissue-based test systems," *Annu. Int.*

Conf. IEEE Eng. Med. Biol. - Proc., vol. 26 III, pp. 2070–2073, 2004.

[4] F. Groeber *et al.*, "Impedance Spectroscopy for the Non-Destructive Evaluation of in Vitro Epidermal Models," *Pharm. Res.*, vol. 32, no. 5, pp. 1845–1854, 2015.

[5] F. Artis, D. Dubuc, J. J. Fournie, M. Poupot, and K. Grenier, "Sub-microliter microwave dielectric spectroscopy for identification and quantification of carbohydrates in aqueous solution," *2015 IEEE Top. Conf. Biomed. Wirel. Technol. Networks, Sens. Syst. BioWireleSS 2015*, pp. 45–47, 2015.

[6] K. Grenier, D. Dubuc, T. Chen, F. Artis, M. Poupot, and J. J. Fournié, "Microwave dielectric spectroscopy: An emerging analyzing technique for biological investigations at the cellular level," *BioWireleSS 2013 - Proc. 2013 IEEE Top. Conf. Biomed. Wirel. Technol. Networks, Sens. Syst. - 2013 IEEE Radio Wirel. Week, RWW 2013*, pp. 40–42, 2013.

[7] G. Poiroux *et al.*, "Label-free detection of mitochondrial activity with Microwave Dielectric Spectroscopy Research Article To cite this version : HAL Id : hal-03027924 International Journal of Biotechnology and Bioengineering Label-free detection of mitochondrial activity wi," 2020.

[8] A. P. O'Rourke *et al.*, "Dielectric properties of human normal, malignant and cirrhotic liver tissue: In vivo and ex vivo measurements from 0.5 to 20 GHz using a precision open-ended coaxial probe," *Phys. Med. Biol.*, vol. 52, no. 15, pp. 4707–4719, 2007.

[9] M. Lazebnik *et al.*, "A large-scale study of the ultrawideband microwave dielectric properties of normal, benign and malignant breast tissues obtained from cancer surgeries," *Phys. Med. Biol.*, vol. 52, no. 20, pp. 6093–6115, 2007.

[10] M. Lazebnik, E. L. Madsen, G. R. Frank, and S. C. Hagness, "Physics in Medicine & Biology Tissue-mimicking phantom materials for narrowband and ultrawideband microwave applications Tissue-mimicking phantom materials for narrowband and ultrawideband microwave applications," 2005.

[11] J. A. Osterberg *et al.*, "Microwave Sensing of Yeast Cell Species and Viability," *IEEE Trans. Microw. Theory Tech.*, vol. 69, no. 3, pp. 1875–1886, 2021.

[12] F. Artis *et al.*, "Microwaving biological cells: Intracellular analysis with microwave dielectric spectroscopy," *IEEE Microw. Mag.*, vol. 16, no. 4, pp. 87–96, 2015.

[13] S. Nath and G. R. Devi, "Three-dimensional culture systems in cancer research: Focus on tumor spheroid model," *Pharmacol. Ther.*, vol. 163, pp. 94–108, 2016.

[14] C. Veelken, G. J. Bakker, D. Drell, and P. Friedl, "Single cell-based automated quantification of therapy responses of invasive cancer spheroids in organotypic 3D culture," *Methods*, vol. 128, pp. 139–149, 2017.

[15] A. Tamra, M. P. Rols, D. Dubuc, and K. Grenier, "Impact of a chemical stimulus on two different cell lines through microwave dielectric spectroscopy at the single cell level," *IEEE MTT-S 2019 Int. Microw. Biomed. Conf. IMBioC 2019 - Proc.*, vol. 1, pp. 1–4, 2019.

[16] A. Tamra, M. Deburghgraeve, D. Dubuc, M. P. Rols, and K. Grenier, "Microwave dielectric spectroscopy for single cell irreversible electroporation monitoring," *IEEE MTT-S Int. Microw. Symp. Dig.*, vol. 2016-Augus, pp. 2–5, 2016.

[17] M. Lazebnik *et al.*, "Highly Accurate Debye Models for Normal and.pdf," vol. 17, no. 12, pp. 822–824, 2007.

[18] E. C. Costa, A. F. Moreira, D. de Melo-Diogo, V. M. Gaspar, M. P. Carvalho, and I. J. Correia, "3D tumor spheroids: an overview on the tools and techniques used for their analysis," *Biotechnol. Adv.*, vol. 34, no. 8, pp. 1427–1441, 2016.

[19] S. Nath and G. R. Devi, "Three-dimensional culture systems in cancer research: Focus on tumor spheroid model," *Pharmacol. Ther.*, vol. 163, pp. 94–108, 2016.

[20] O. Peytral-Rieu, K. Grenier, and D. Dubuc, "Microwave Sensor Dedicated to the Determination of the Dielectric Properties of 3D Biological Models from 500MHz to 20GHz," *IEEE MTT-S Int. Microw. Symp. Dig.*, vol. 2021-June, pp. 222–225, 2021.

[21] N. J. M. C. Mortensen and J. F. Morris, "The effect of fixation conditions on the ultrastructural appearance of gastrin cell granules in the rat gastric pyloric antrum," *Cell Tissue Res.*, vol. 176, no. 2, pp. 251–263, 1977.

[22] J. Virtanen, H. Uusital, A. Palkama, and H. Kaufman, "the Effect of Fixation on and Morphology in Scanning Electron Microscopy," *Acta Ophtalmol.*, vol. 62, pp. 577–585, 1984.